



Research paper

Distal denervation in the SOD1 knockout mouse correlates with loss of mitochondria at the motor nerve terminal

Lindsey R. Hayes^{c,*}, Seneshaw A. Asress^{a,1}, Yingjie Li^a, Alexander Galkin^d, Anna Stepanova^d, Hibiki Kawamata^d, Giovanni Manfredi^d, Jonathan D. Glass^{a,b}

^a Department of Neurology and Center for Neurodegenerative Disease, Emory University, Atlanta, GA 30322, USA

^b Department of Pathology and Laboratory Medicine, Emory University, Atlanta, GA 30322, USA

^c Department of Neurology, Johns Hopkins University, Baltimore, MD 21205, USA

^d Feil Family Brain and Mind Research Institute, Weill Cornell Medicine, New York, NY 10065, USA



ARTICLE INFO

Keywords:

Superoxide dismutase-1

Oxidative stress

Axonal degeneration

Mitochondria

Neuromuscular junction

Amyotrophic lateral sclerosis

ABSTRACT

Impairment of mitochondrial transport has long been implicated in the pathogenesis of neuropathy and neurodegeneration. However, the role of mitochondria in stabilizing motor nerve terminals at neuromuscular junction (NMJ) remains unclear. We previously demonstrated that mice lacking the antioxidant enzyme, superoxide dismutase-1 (*Sod1*^{-/-}), develop progressive NMJ denervation. This was rescued by expression of SOD1 exclusively in the mitochondrial intermembrane space (*MitoSOD1/Sod1*^{-/-}), suggesting that oxidative stress within mitochondria drives denervation in these animals. However, we also observed reduced mitochondrial density in *Sod1*^{-/-} motor axons in vitro. To investigate the relationship between mitochondrial density and NMJ innervation in vivo, we crossed *Sod1*^{-/-} mice with the fluorescent reporter strains *Thy1-YFP* and *Thy1-mitoCFP*. We identified an age-dependent loss of mitochondria at motor nerve terminals in *Sod1*^{-/-} mice, that closely correlated with NMJ denervation, and was rescued by *MitoSOD1* expression. To test whether augmenting mitochondrial transport rescues *Sod1*^{-/-} axons, we generated transgenic mice overexpressing the mitochondrial cargo adaptor, *Miro1*. This led to a partial rescue of mitochondrial density at motor nerve terminals by 12 months of age, but was insufficient to prevent denervation. These findings suggest that loss of mitochondria in the distal motor axon may contribute to denervation in *Sod1*^{-/-} mice, perhaps via loss of key mitochondrial functions such as calcium buffering and/or energy production.

1. Introduction

Motor nerve terminals at the neuromuscular junction (NMJ) have long been known to have a high density of mitochondria (de Harven and Coërs, 1959). Synaptic mitochondria have numerous vital functions including ATP production and maintenance of calcium homeostasis (David and Barrett, 2003). Neuronal mitochondria undergo dynamic trafficking to sites of metabolic demand, such as synapses and nodes of Ranvier (Hollenbeck, 1996). Mutations that impair mitochondrial dynamics, either through disruption of axonal transport or fission and fusion, are an important cause of hereditary peripheral neuropathies (Baloh, 2008). Abnormal mitochondrial trafficking is also reported in neurodegenerative disorders such as amyotrophic lateral sclerosis (ALS) (De Vos et al., 2007; Magrané et al., 2014). However, the specific cause of impaired mitochondrial trafficking in ALS, and the consequences for

NMJ stability, are poorly understood.

Superoxide dismutase-1 (SOD1) is an antioxidant enzyme that neutralizes superoxide radical, produced as a byproduct of mitochondrial electron transport (McCord and Fridovich, 1969). Data from SOD1 loss-of-function (SOD1 knockout, *Sod1*^{-/-}) (Fischer et al., 2012; Jang et al., 2009), and gain-of-function models (SOD1 mutant models of familial ALS) (Fischer et al., 2004; Frey et al., 2000), show progressive denervation at the NMJ, illustrating the importance of SOD1 for NMJ stability in aging and motor neuron disease. Whereas the SOD1 mutant ALS models show widespread spinal motor neuron death by endstage, the *Sod1*^{-/-} mouse develops a milder motor neuropathy, in which the pathology is restricted to the distal motor axon, and no loss of ventral root axons or motor neurons is seen even at advanced ages (Fischer et al., 2012). Therefore, the *Sod1*^{-/-} mouse is a useful model for studying the events leading to NMJ denervation in the context of

* Corresponding author at: Johns Hopkins School of Medicine, 855 N. Wolfe St, Suite 229, Baltimore, MD 21205, USA.

E-mail address: lhayes@jhmi.edu (L.R. Hayes).

¹ L.R.H. and S.A.A. contributed equally to this work.

<https://doi.org/10.1016/j.expneurol.2019.05.008>

Received 7 February 2019; Received in revised form 3 May 2019; Accepted 8 May 2019

Available online 10 May 2019

0014-4886/© 2019 Elsevier Inc. All rights reserved.

chronic oxidative stress.

Although SOD1 is commonly regarded as a cytoplasmic enzyme, it is also found in the mitochondrial intermembrane space (IMS), the primary site of superoxide radical release (Sturtz et al., 2001). Moreover, oxidative stress in *Sod1*^{-/-} models appears preferentially targeted to mitochondria (Aquilano et al., 2006; Jang et al., 2009; Muller et al., 2007; Yanase et al., 2009). When we replaced SOD1 exclusively within the mitochondrial intermembrane space of the knockout mice (*MitoSOD1/Sod1*^{-/-}), this was sufficient to prevent NMJ denervation (Fischer et al., 2011). These data raised the important question of the role of mitochondria, and specifically mitochondrial SOD1, in the maintenance of the NMJ. When we examined mitochondrial density in *Sod1*^{-/-} motor axons in vitro, we found that the density was reduced, and this was correlated with reduced axon outgrowth (Fischer et al., 2012). These in vitro data led to the hypothesis that oxidative stress-mediated impairment of mitochondrial transport, and subsequent reduction of mitochondrial density in axons, may lead to denervation at the NMJ.

To test this hypothesis in vivo, we crossed *Sod1*^{-/-} mice with a *Thy1-mitoCFP* reporter mouse and analyzed mitochondrial density in motor nerve terminals. We observed a progressive loss of presynaptic mitochondria at *Sod1*^{-/-}/*Thy1-mitoCFP* NMJs, which preceded denervation. This was rescued by mitoSOD1, suggesting that mitochondrial oxidative stress indeed disrupts mitochondrial localization in this model. To test whether augmenting mitochondrial transport prevents denervation, we generated mice overexpressing the mitochondrial cargo adaptor, Miro1. When crossed with *Sod1*^{-/-} mice, Miro1 overexpression conferred only a modest rescue of presynaptic mitochondrial density at 12 months of age, but did not protect against denervation. Taken together, our data demonstrate that oxidative stress leads to loss of mitochondria at motor nerve terminals in vivo, and supports the hypothesis that mitochondria play an essential role in maintenance of the NMJ. Further studies are needed to determine the mechanism by which oxidative stress alters mitochondrial transport and/or turnover in axons, and identify strategies for intervention.

2. Material and methods

2.1. Animals

All animal experiments were in compliance with the Emory University Institutional Animal Care and Use Committee. *Sod1*^{-/-}, *Thy1-YFP16*, and *MitoSOD1* mice were obtained as previously described (Fischer et al., 2011). *Thy1-MitoCFP* mice expressing CFP fused to the human cytochrome c oxidase mitochondrial targeting sequence were from Jackson Laboratories (Misgeld et al., 2007). All transgenic lines were on a C57BL/6 background, except for *MitoSOD1*, which were on a B6SJL background. Genotyping was by standard PCR analysis on tail snip DNA. *Thy1-YFP16* mice were identified by examination of epidermal nerve fibers in ear punches.

2.2. Miro1 plasmids and transgenic mice

The human Miro1 plasmid was generously provided by Pontus Aspenstrom (Fransson et al., 2003). To generate Miro1 transgenic mice, an N-terminal 3xFLAG tag (Sigma) was added prior to insertion into a *Thy1.2* expression cassette (Addgene) (Caroni, 1997). *Thy1-3xFLAG-Miro1* transgenic mice were generated by pronuclear injection into fertilized eggs of C57BL/6 mice (Emory Transgenic Mouse and Gene Targeting Core Facility). Seven founders were identified by PCR, with the following primers: 5'-GAGTTGGGAAGACATCCTG-3' (forward) and 5'-AGTAGTTTCGTGTCTCCCTC-3' (reverse) to generate a 620 bp product. The line with the highest level of expression by anti-FLAG Western blot was subsequently used for breeding with *Sod1*^{-/-} mice. Motor neuron expression was also verified in paraffin-embedded sections of the lumbar spinal cord by FLAG immunohistochemistry.

2.3. Neuromuscular junction analysis

Mice were sacrificed and perfused with 4% paraformaldehyde, and 30 μ m frozen sections of tibialis anterior muscles prepared as previously described (Fischer et al., 2004). Acetylcholine receptors at the motor endplate were labeled with Alexa Fluor 555-conjugated α -bungarotoxin (BTX) (Invitrogen), 1:3000 in PBS (30 min). Motor axon terminals were identified by YFP, and axonal mitochondria by CFP. Innervated, partially denervated, and denervated endplates were defined by complete, partial or absent overlap between nerve terminal and endplate, respectively. Presence or absence of mitochondria was scored only in terminals with partial or full overlap of endplates. Examiners were blinded to genotypes. All endplates were evaluated in every fourth section.

2.4. Primary motor neuron culture

Spinal motor neurons were enriched from wild-type E12.5 mouse embryos by density centrifugation as previously described (Fischer et al., 2011). Two days after plating, cells were co-transfected with dsred-Mito (Clontech) and either Miro1-GFP or GFP alone using NeuroMag beads (Oz Biosciences) as described (Fallini et al., 2010). Live cell imaging of mitochondrial transport was done on a Nikon A1R confocal microscope with a heat- and CO₂-controlled stage. Images were collected every 5 s for 5 min using a 60 \times oil objective. Kymographs were processed and analyzed using ImageJ (Miller and Sheetz, 2004). Mitochondria were considered mobile if displaced $\geq 5 \mu$ m (Kang et al., 2008).

2.5. Mitochondrial fractionation and Western blot

Spinal cord and sciatic nerves were collected in 10 mM Tris, pH 7.4, 320 mM sucrose, and 20% DMSO and snap frozen in liquid nitrogen. For mitochondrial isolation, tissues were homogenized in MSE buffer (225 mM mannitol, 75 mM sucrose, 5 mM HEPES, 0.1% BSA, 1 mM EGTA, 0.1 mM EDTA pH 8.0), using a dounce homogenizer (Wheaton). Tissue debris was discarded after centrifugation for 4 min at 1500 g, and the supernatant was spun for 15 min at 20,000 g. The pellet was rinsed twice with SET buffer (50 mM Tris-HCl pH 7.5, 0.25 M sucrose, and 0.2 mM EDTA), and the resulting mitochondria-enriched pellet was resuspended in SET buffer, frozen and stored at -80°C until use. Proteins were separated by SDS-PAGE according to standard protocols, and transferred onto nitrocellulose membranes with the Trans Blot Turbo system (Bio-Rad). Primary antibodies included: Miro1 (Novus, 1:1000), MFN2 (Sigma, 1:1000), TIM23 (BD Biosciences, 1:5000), and FLAG (Sigma M2, 1:1000). Blots were visualized with enhanced chemiluminescence on the Chemidoc Touch (Bio-Rad), and quantified using Image Lab software (Bio-Rad).

3. Results

3.1. Mitochondrial loss in presynaptic motor terminals in *Sod1*^{-/-} mice

We previously demonstrated that *Sod1*^{-/-} primary motor neurons show reduced axonal mitochondrial density (Fischer et al., 2011, 2012). To evaluate the density of mitochondria at motor nerve terminals in vivo, we crossed *Sod1*^{-/-} mice with fluorescent reporter mice expressing *Thy1-YFP* (to label axons), and *Thy1-mitoCFP* (to label mitochondria, Fig. 1A). At 4, 12, and 20 months of age, NMJ innervation (fully denervated, partially innervated, and fully innervated terminals) and the presence or absence of mitochondria in motor nerve terminals were scored in tibialis anterior muscle. Mitochondria were scored only in partially or fully innervated terminals.

As we previously reported, by 4 months of age, *Sod1*^{-/-} mice develop NMJ denervation, that worsens over time (Fig. 1B, note: only fully denervated endplates are shown). In 4-month-old *Sod1*^{-/-} mice,

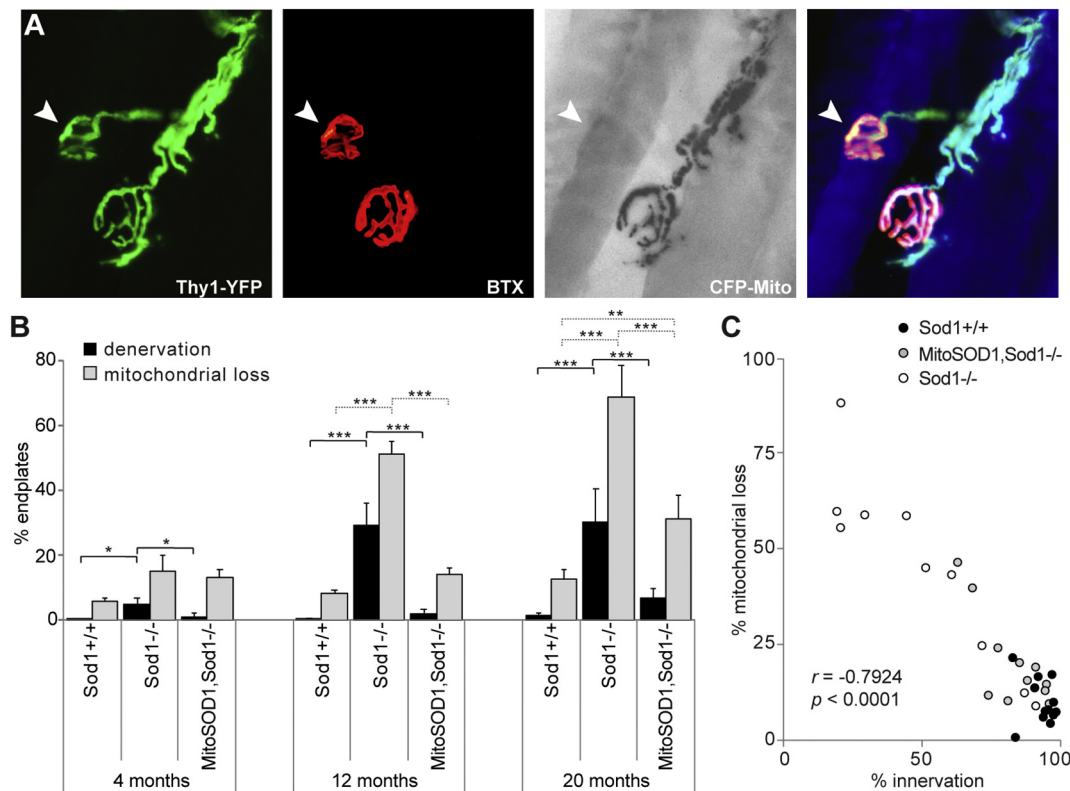


Fig. 1. Mitochondrial loss at the NMJ in *Sod1*^{-/-} mice correlates with denervation and is rescued by MitoSOD1. (A) Representative innervated NMJs from *Sod1*^{-/-} tibialis anterior muscle, one of which lacks CFP-labeled mitochondria (arrow). The motor endplate (α -bungarotoxin) is labeled in red, motor axon (YFP) in green and mitochondria (CFP) in grayscale. (B) Percent fully denervated endplates vs. mitochondrial loss among innervated and partially innervated endplates. $N = 3$ –6 animals per group. 300–600 endplates were assessed per muscle. Values are mean \pm SEM (* $p < .05$, ** $p < .01$, *** $p < .001$, two-way ANOVA with Tukey post-hoc). (C) Correlation between percent mitochondrial loss and NMJ innervation, across all ages and genotypes (Spearman's $r = -0.7924$, $p < .0001$, $n = 35$). (For interpretation of the references to colour in this figure legend, the reader is referred to the web version of this article.)

a trend toward increasing mitochondrial loss was seen, with 15.3% of *Sod1*^{-/-} NMJs devoid of mitochondria, increasing to 51% at 12 months ($p < .0001$) and 68% at 20 months ($p < .0001$). This was in contrast to *Sod1*^{+/+} littermates, where the proportion of nerve terminals lacking mitochondria increased only minimally with aging, from 6.1% at 4 months, to 12.6% at 20 months. In addition to preserving innervation, replacement of SOD1 in the mitochondrial IMS (*MitoSOD1*/*Sod1*^{-/-}) normalized mitochondrial density at 4 and 12 months (n.s. versus *Sod1*^{+/+}), and significantly reduced mitochondrial loss at 20 months (68.7% for *Sod1*^{-/-}, versus 31.1% for *MitoSOD1*/*Sod1*^{-/-}, $p < .0001$). When mitochondrial loss was plotted against endplate innervation, across all genotypes, a strong negative correlation was observed (Fig. 1C, Spearman's $r = -0.7924$, $p < .001$). These data demonstrate age-dependent loss of mitochondria at *Sod1*^{-/-} motor nerve terminals that is rescued by expression of SOD1 in the mitochondrial IMS. These findings suggest that oxidative stress impairs axonal mitochondrial dynamics in vivo, which may contribute to NMJ denervation.

3.2. Mitochondrial transport proteins are unaffected by loss of SOD1

The distribution of mitochondria in neurons is dependent on multiple processes including retrograde and anterograde transport, fusion, and fission. For example, the outer membrane protein, Miro1 (mitochondrial Rho GTPase), plays an essential role in microtubule-mediated fast axonal transport of mitochondria (Fransson et al., 2003, 2006), and Mitofusin 2 (MFN2), also on the outer mitochondrial membrane, is critical for mitochondrial fusion and motility (Misko et al., 2010). Mutation of both of these proteins has been linked to neurodegeneration (Baloh et al., 2007; Nguyen et al., 2014). We

hypothesized that these key mitochondrial proteins may undergo oxidative stress-mediated damage in *Sod1*^{-/-} mice, resulting in abnormal mitochondrial dynamics. However, levels of Miro1 and MFN2, as well as the inner membrane protein TIM23 were unaltered in spinal cord (Fig. 2A–D) and sciatic nerve homogenates (not shown) from *Sod1*^{-/-} mice, including mitochondrial fractions. Thus, depletion of mitochondrial transport proteins is unlikely to contribute to the abnormal mitochondrial distribution in *Sod1*^{-/-} mice, though we were unable to specifically isolate mitochondria located at the nerve terminal.

3.3. Miro1 increases mitochondrial movement and attenuates mitochondrial loss at the NMJ

Next, we investigated whether augmenting mitochondrial transport could rescue NMJ denervation in *Sod1*^{-/-} mice. In *Drosophila*, overexpression of dMiro leads to accumulation of mitochondria at the NMJ, while knocking it out causes mitochondrial retention in motor neuron cell bodies (Guo et al., 2005). In rat hippocampal neurons, overexpression of human Miro1 increases anterograde and retrograde movement of mitochondria, and results in increased mitochondrial density in neuronal processes (MacAskill et al., 2009a, 2009b). To test whether Miro1 overexpression increases mitochondrial movement in motor neurons, we co-transfected primary motor neurons with Miro1 and a fluorescent mitochondrial tag (dsred-Mito) and monitored mitochondrial movement by live imaging. As was reported in hippocampal neurons, overexpression of Miro1 increased mitochondrial movement by over two-fold (Fig. 3A–B). The frequency of anterograde vs. retrograde movement was not altered (Fig. 3C).

To evaluate the protective effect of Miro1 in vivo, we generated

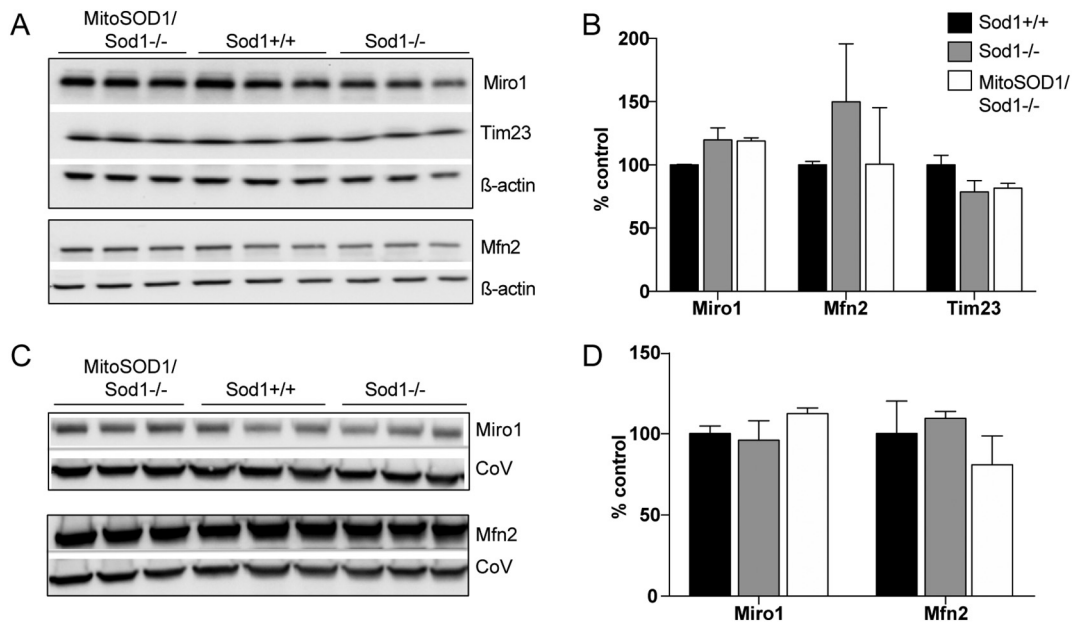


Fig. 2. Mitochondrial transport protein levels are unaffected by loss of SOD1. (A–B) Western blots of spinal cord homogenates, probed for Miro1, Tim23, and Mfn2. (B) Densitometry for the blots in A, normalized to β -actin loading control. (C) Western blots of spinal cord mitochondrial fractions, probed for Mfn2 and Miro1. (D) Densitometry for the blots in C, shown as percent ATPase subunit β (CoV) loading control. $N = 3$ mice per genotype. Values are mean \pm SEM. No significant differences were observed between genotypes.

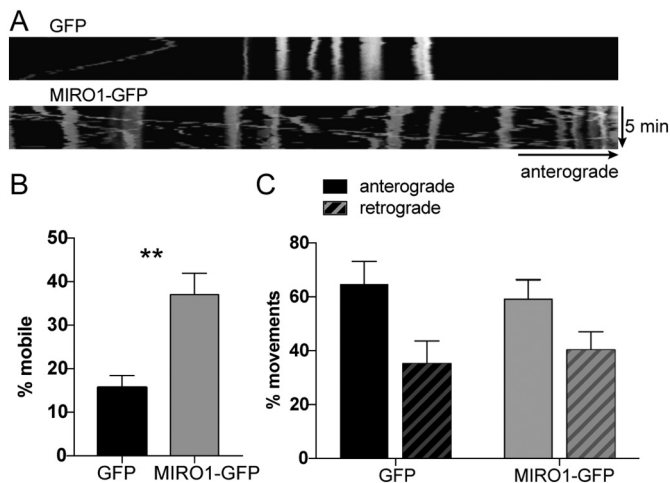


Fig. 3. Miro1 increases mitochondrial mobility in motor axons. (A) Representative kymographs depicting axonal transport of dsRed-Mito labeled mitochondria in wild type primary motor neurons cotransfected with GFP (top) or Miro1-GFP (bottom). (B) Percent mobile mitochondria. (C) Percent mitochondrial movements that were in the anterograde versus retrograde direction. Solid bars indicate anterograde transport, hashed bars indicate retrograde transport. $N = 10$ axons (248 mitochondria) for GFP, $n = 8$ axons (214 mitochondria) for Miro-GFP (** $p < .01$, Student's t -test).

transgenic mice overexpressing human Miro1, under the control of the pan-neuronal Thy1 promoter (Fig. 4A). Given the lack of specific antibodies to distinguish human and mouse Miro1, we added a 3 \times -FLAG tag. Multiple transgenic lines were generated, and the line with the highest expression was selected for further studies. In this line, robust overexpression was seen by anti-FLAG Western blot and immunohistochemistry in spinal cord and sciatic nerve (Fig. 4B, C), as well as by anti-MIRO1 Western (Fig. 4D). Miro1-overexpressing mice were crossed with *Sod1*^{-/-} mice (expressing the Thy1-YFP and -MitoCFP reporters), and NMJ innervation and mitochondrial density were again analyzed in tibialis anterior muscle.

At 4 months, no apparent benefit of Miro1 overexpression was seen

(Fig. 4E). At 12 months, there was a 22% increase in the percent of motor nerve terminals with mitochondria ($p = .0260$), accompanied by a trend toward reduced denervation (29.5% denervation in *Sod1*^{-/-}, versus 17.6% in *Miro1/Sod1*^{-/-}), although this did not reach statistical significance.

4. Discussion

Denervation at the NMJ disrupts communication between spinal motor neurons and their target muscles, leading to muscle weakness and atrophy. Understanding mechanisms of NMJ denervation in aging and disease is therefore important for developing therapeutic strategies. In this study, we demonstrate progressive loss of presynaptic mitochondria at the NMJ in the *Sod1*^{-/-} mouse, a model of increased oxidative stress. Evacuation of mitochondria from the nerve terminal, along with NMJ innervation, is rescued by replacement of SOD1 in the mitochondrial IMS, but not by overexpression of the mitochondrial transport adaptor, Miro1. These findings confirm our earlier in vitro findings and support the hypothesis that chronic oxidative stress leads to depletion of mitochondria at the nerve terminal. This may in turn contribute to denervation, perhaps via loss of key mitochondrial functions such as calcium buffering and/or energy production.

4.1. Oxidative stress impairs mitochondrial dynamics

Mitochondrial distribution within axons is controlled by a complex interplay between anterograde and retrograde axonal transport, fission, fusion, and mitophagy. There is growing evidence that oxidative stress may disrupt these processes at multiple levels. In primary rat hippocampal cultures, application of hydrogen peroxide directly to axons, using microfluidic chambers, rapidly inhibits both anterograde and retrograde mitochondrial transport (Fang et al., 2012). In *Drosophila*, exposure to the superoxide-generating herbicide, paraquat, slows transport of mitochondria but not dense core vesicles, and also reduces mitochondrial size consistent with fission-fusion disruption (Liao et al., 2017). We previously demonstrated that at 4 months, the redox state of glutathione, a major intracellular redox buffer in cells, is significantly oxidized in tibial nerve from *Sod1*^{-/-} mice (Fischer et al., 2012). We

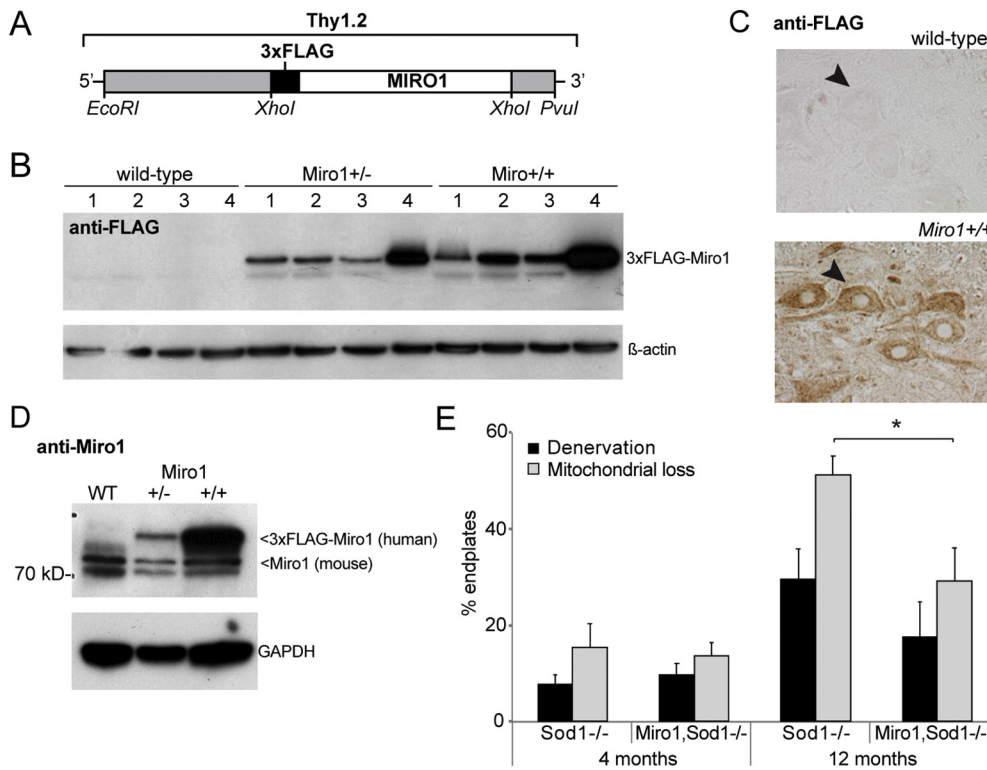


Fig. 4. Mirol overexpression modestly increases mitochondrial density at the NMJ but does not prevent denervation. (A) Schematic of the Thy1-3xFLAG-Miro1 construct used to generate human Mirol-overexpressing mice. (B) Anti-FLAG Western blot showing 3xFLAG-Miro1 expression in spinal cord and sciatic nerve (1 = proximal sciatic nerve, 2 = mid-sciatic nerve, 3 = distal sciatic nerve, 4 = spinal cord). (C) Anti-FLAG immunohistochemistry. Representative images of the ventral horn of lumbar spinal cord are shown (arrow = motor neuron). (D) Anti-Miro1 Western blot showing 3xFLAG-Miro1 expression in spinal cord. (E) Percent fully denervated endplates and mitochondrial loss at tibialis anterior NMJs in *Sod1*^{-/-} versus *Miro1/Sod1*^{-/-} mice at 4 and 12 months of age. Values are mean ± SEM. At 4 months, *n* = 10 *Sod1*^{-/-} and *n* = 8 *Miro1/Sod1*^{-/-} mice were used for innervation and *n* = 3 mice per genotype for mitochondrial analysis. At 12 months, *n* = 4 *Sod1*^{-/-} and *n* = 5 *Miro1/Sod1*^{-/-} mice were used for both parameters. **p* < .05, two-way ANOVA with Tukey post-hoc analysis.

also analyzed the redox state of cytoplasmic (TRX1) vs. mitochondrial (TRX2) thioredoxin in primary *Sod1*^{-/-} neurons, and observed selective oxidation of TRX2 (Fischer et al., 2011). Here, we hypothesized that excess mitochondrial ROS in this model may damage key mitochondrial regulatory proteins to disrupt transport. However, levels of Mirol, MFN2, and TIM23 were unchanged in *Sod1*^{-/-} spinal cord and sciatic nerve. These proteins may still be oxidatively modified, without changes in their expression level. Or, changes may be isolated to nerve terminals, since the mitochondrial loss we observe is very distal. In addition to altered transport, ROS-induced mitochondrial membrane depolarization has also been shown to trigger mitophagy (Wang et al., 2014), which could lead to accelerated degradation of mitochondria at nerve terminals. In support of this, SOD1-G93A mice show abnormal mitophagy activation, which is rescued by ablation of Parkin, slowing denervation and prolonging survival in these mice (Palomo et al., 2018). Mitophagy warrants further study in the *Sod1*^{-/-} model as a potential mechanism of mitochondrial loss at nerve terminals.

4.2. Loss of mitochondria and NMJ denervation

The loss of mitochondria at motor nerve terminals in *Sod1*^{-/-} mice closely parallels the time course of NMJ denervation. Additional studies are needed to determine whether depletion of mitochondria from nerve terminals directly results in denervation. Mitochondria are normally highly enriched at the presynaptic motor nerve terminal, where they are presumed to be critical for ATP production and calcium buffering (Ly and Verstreken, 2006). However, studies looking at the consequences of mitochondrial transport disruption in *Drosophila* and mouse models show conflicting results. *Drosophila* larvae lacking dMirol and Milton show striking absence of mitochondria at the NMJ with accumulation at the cell body (Guo et al., 2005; Stowers et al., 2002). However, NMJ innervation and basal signaling is maintained, with deficits only at high frequency stimulation. In contrast, *Miro1*^{-/-} mice die at birth due to lack of respiration, attributed to failure of development of cranial and cervical motor neurons (Nguyen et al., 2014).

Conditional knockout of Mirol in cortical, hippocampal, and spinal cord neurons (via the neuron-specific enolase 2 promoter) causes progressive neurological dysfunction and death by postnatal day 35. NMJs were not evaluated in these mice, however reduced mitochondrial density was seen in corticospinal tract axons. MFN2 knockout is also embryonic lethal (Misko et al., 2010), and MFN2 mutations associated with CMT2A severely impair mitochondrial transport (Baloh et al., 2007) and cause motor axon degeneration (Detmer et al., 2007). These studies suggest that in mice, as opposed to *Drosophila*, primary impairment of mitochondrial transport is sufficient to trigger axonal degeneration.

4.3. Role of Mirol in motor axons

Guo and colleagues found that neuronal overexpression of *Drosophila* dMirol resulted in a significant increase in the density of mitochondria in distal motor axons (Guo et al., 2005), whereas we found only a modest improvement in mitochondrial density in *Sod1*^{-/-} nerve terminals. There was also a trend toward reduced denervation, however our study was insufficiently powered to detect subtle changes (*n* = 18 mice per group would have been required). Perhaps the level of Mirol expression was not high enough to overcome ROS-mediated transport impairment. In addition, our data from primary motor neurons suggest that although Mirol overexpression increases mitochondrial mobility, this occurs in both the anterograde and retrograde direction. Unlike *Drosophila*, there are two isoforms of Mirol (Mirol and Mirol2) in mammals. The severe motor degenerative phenotype seen in *Miro1* knockout mice supports the idea that Mirol1 plays an important role in motor neurons (Nguyen et al., 2014). However, siRNA experiments in primary dorsal root ganglia sensory neurons show that Mirol2 plays a more important role in mitochondrial transport in these cells (Misko et al., 2010). Further studies are needed to understand cell- and isoform-specific roles for Mirol1 and Mirol2 in motor vs. sensory axons.

4.4. Mitochondrial transport dysfunction and motor neuron disease

In addition to mitofusins mutations in CMT2A, impaired mitochondrial transport in motor neurons has also received significant attention in ALS (Magrané and Manfredi, 2009). Miro1 expression has been shown to be reduced in the spinal cord of patients with sporadic ALS, as well as *SOD1-G93A* and TDP43 M337V mutant mice (Zhang et al., 2015; Palomo et al., 2018), suggesting a potential role for loss of Miro1 in impaired mitochondrial transport in ALS. As in *Sod1*^{-/-} mice, we have also observed early loss of mitochondria at *SOD1-G93A* motor nerve terminals, but crossing these animals with our Miro1 overexpressing line did not rescue the phenotype (*not shown*). Similarly, when Zhu and colleagues knocked out syntaphilin, a mitochondrial docking protein, in *SOD1-G93A* mice, they saw an increase in anterograde and retrograde mitochondrial transport but no motor neuron rescue or change in survival (Zhu and Sheng, 2011). Perhaps, as in *Sod1*^{-/-} mice, improving mitochondrial transport alone without also correcting other insults, such as oxidative stress and/or activation of mitophagy, is insufficient to prevent motor pathology.

5. Conclusion

We have identified an age-dependent loss of mitochondria at the NMJ in *Sod1*^{-/-} mutant mice, that strongly correlates with NMJ denervation. This defect was rescued by expression of SOD1 in the mitochondrial IMS, supporting the idea that the abnormal mitochondrial distribution in this model is due to oxidative stress. Manipulation of transport via Miro1 overexpression was insufficient to rescue NMJs. Additional studies are needed to precisely determine how loss of SOD1 affects mitochondrial dynamics in axons and identify targets for intervention.

Acknowledgements

This work was supported by the Muscular Dystrophy Association (JG), NIH 1R01NS062055 (GM), and an AAN/ALSA Clinician Scientist Development award (LH).

The authors declare no competing financial interests.

References

- Aquilano, K., Vigilanza, P., Rotilio, G., Ciriolo, M.R., 2006. Mitochondrial damage due to SOD1 deficiency in SH-SY5Y neuroblastoma cells: a rationale for the redundancy of SOD1. *FASEB J.* 20, 1683–1685. <https://doi.org/10.1096/fj.05-5225fje>.
- Baloh, R.H., 2008. Mitochondrial dynamics and peripheral neuropathy. *Neuroscientist* 14, 12–18. <https://doi.org/10.1177/1073858407307354>.
- Baloh, R.H., Schmidt, R.E., Pestronk, A., Milbrandt, J., 2007. Altered axonal mitochondrial transport in the pathogenesis of Charcot-Marie-Tooth disease from mitofusins 2 mutations. *J. Neurosci.* 27, 422–430. <https://doi.org/10.1523/JNEUROSCI.4798-06.2007>.
- Caroni, P., 1997. Overexpression of growth-associated proteins in the neurons of adult transgenic mice. *J. Neurosci. Methods* 71, 3–9. [https://doi.org/10.1016/S0165-0270\(96\)00121-5](https://doi.org/10.1016/S0165-0270(96)00121-5).
- David, G., Barrett, E.F., 2003. Mitochondrial Ca²⁺ uptake prevents desynchronization of quantal release and minimizes depletion during repetitive stimulation of mouse motor nerve terminals. *J. Physiol.* 548, 425–438. <https://doi.org/10.1113/jphysiol.2002.035196>.
- de Harven, E., Coërs, C., 1959. Electron microscope study of the human neuromuscular junction. *J. Biophys. Biochem. Cytol.* 6, 7–10.
- De Vos, K.J., Chapman, A.L., Tennant, M.E., Manser, C., Tudor, E.L., Lau, K.F., Brownlees, J., Ackerley, S., Shaw, P.J., McLoughlin, D.M., Shaw, C.E., Leigh, P.N., Miller, C.C.J., Grierson, A.J., 2007. Familial amyotrophic lateral sclerosis-linked SOD1 mutants perturb fast axonal transport to reduce axonal mitochondria content. *Hum. Mol. Genet.* 16, 2720–2728. <https://doi.org/10.1093/hmg/ddm226>.
- Detmer, S.A., Velde, C.V., Cleveland, D.W., Chan, D.C., 2007. Hindlimb gait defects due to motor axon loss and reduced distal muscles in a transgenic mouse model of Charcot-Marie-Tooth type 2A. *Hum. Mol. Genet.* 17, 367–375. <https://doi.org/10.1093/hmg/ddm314>.
- Fallini, C., Bassell, G.J., Rossoll, W., 2010. High-efficiency transfection of cultured primary motor neurons to study protein localization, trafficking, and function. *Mol. Neurodegener.* 5, 17. <https://doi.org/10.1186/1750-1326-5-17>.
- Fang, C., Bourdette, D., Banker, G., 2012. Oxidative stress inhibits axonal transport: implications for neurodegenerative diseases. *Mol. Neurodegener.* 7, 29. <https://doi.org/10.1186/1750-1326-7-29>.
- Fischer, L.R., Culver, D.G., Tennant, P., Davis, A.A., Wang, M., Castellano-Sanchez, A., Khan, J., Polak, M.A., Glass, J.D., 2004. Amyotrophic lateral sclerosis is a distal axonopathy: evidence in mice and man. *Exp. Neurol.* 185, 232–240. <https://doi.org/10.1016/j.expneurol.2003.10.004>.
- Fischer, L.R., Igoudjil, A., Magrane, J., Li, Y., Hansen, J.M., Manfredi, G., Glass, J.D., 2011. SOD1 targeted to the mitochondrial intermembrane space prevents motor neuropathy in the *Sod1* knockout mouse. *Brain* 134, 196–209. <https://doi.org/10.1093/brain/awq314>.
- Fischer, L.R., Li, Y., Asress, S.A., Jones, D.P., Glass, J.D., 2012. Absence of SOD1 leads to oxidative stress in peripheral nerve and causes a progressive distal motor axonopathy. *Exp. Neurol.* 233, 163–171. <https://doi.org/10.1016/j.expneurol.2011.09.020>.
- Fransson, A., Ruusala, A., Aspenström, P., 2003. Atypical Rho GTPases have roles in mitochondrial homeostasis and apoptosis. *J. Biol. Chem.* 278, 6495–6502. <https://doi.org/10.1074/jbc.M208609200>.
- Fransson, Å., Ruusala, A., Aspenström, P., 2006. The atypical Rho GTPases Miro-1 and Miro-2 have essential roles in mitochondrial trafficking. *Biochem. Biophys. Res. Commun.* 344, 500–510. <https://doi.org/10.1016/j.bbrc.2006.03.163>.
- Frey, D., Schneider, C., Xu, L., Borg, J., Sporeen, W., Caroni, P., 2000. Early and selective loss of neuromuscular synapse subtypes with low sprouting competence in motor neuron diseases. *J. Neurosci.* 20, 2534–2542.
- Guo, X., Macleod, G.T., Wellington, A., Hu, F., Panchumarthi, S., Schoenfeld, M., Marin, L., Charlton, M.P., Atwood, H.L., Zinsmaier, K.E., 2005. The GTPase dMiro1s required for axonal transport of mitochondria to Drosophila synapses. *Neuron* 47, 379–393. <https://doi.org/10.1016/j.neuron.2005.06.027>.
- Hollenbeck, P.J., 1996. The pattern and mechanism of mitochondrial transport in axons. *Front. Biosci.* 1, d91–102.
- Jang, Y.C., Lustgarten, M.S., Liu, Y., Muller, F.L., Bhattacharya, A., Liang, H., Salmon, A.B., Brooks, S.V., Larkin, L., Hayworth, C.R., Richardson, A., Van Remmen, H., 2009. Increased superoxide in vivo accelerates age-associated muscle atrophy through mitochondrial dysfunction and neuromuscular junction degeneration. *FASEB J.* <https://doi.org/10.1096/fj.09-146308>.
- Kang, J.-S., Tian, J.-H., Pan, P.-Y., Zald, P., Li, C., Deng, C., Sheng, Z.-H., 2008. Docking of axonal mitochondria by syntaphilin controls their mobility and affects short-term facilitation. *Cell* 132, 137–148. <https://doi.org/10.1016/j.cell.2007.11.024>.
- Liao, P.-C., Tandarich, L.C., Hollenbeck, P.J., 2017. ROS regulation of axonal mitochondrial transport is mediated by Ca²⁺ and JNK in Drosophila. *PLoS One* 12, e0178105. <https://doi.org/10.1371/journal.pone.0178105>.
- Ly, C.V., Verstreken, P., 2006. Mitochondria at the synapse. *Neuroscientist* 12, 291–299. <https://doi.org/10.1177/1073858406287661>.
- MacAskill, A.F., Brickley, K., Stephenson, F.A., Kittler, J.T., 2009a. GTPase dependent recruitment of Grif-1 by Miro1 regulates mitochondrial trafficking in hippocampal neurons. *Mol. Cell. Neurosci.* 40, 301–312. <https://doi.org/10.1016/j.mcn.2008.10.016>.
- MacAskill, A.F., Rinholm, J.E., Twelvetrees, A.E., Arancibia-Carcamo, I.L., Muir, J., Fransson, Å., Aspenström, P., Attwell, D., Kittler, J.T., 2009b. Miro1 is a calcium sensor for glutamate receptor-dependent localization of mitochondria at synapses. *Neuron* 61, 541–555. <https://doi.org/10.1016/j.neuron.2009.01.030>.
- Magrané, J., Manfredi, G., 2009. Mitochondrial function, morphology, and axonal transport in amyotrophic lateral sclerosis. *Antioxid. Redox Signal.* 11, 1615–1626. <https://doi.org/10.1089/ARS.2009.2604>.
- Magrané, J., Cortez, C., Gan, W.-B., Manfredi, G., 2014. Abnormal mitochondrial transport and morphology are common pathological denominators in SOD1 and TDP43 ALS mouse models. *Hum. Mol. Genet.* 23, 1413–1424. <https://doi.org/10.1093/hmg/ddt528>.
- McCord, J.M., Fridovich, I., 1969. Superoxide dismutase an enzymatic function for erythrocyte hemocuprein. *J. Biol. Chem.* 244, 6049–6055.
- Miller, K.E., Sheetz, M.P., 2004. Axonal mitochondrial transport and potential are correlated. *J. Cell Sci.* 117, 2791–2804. <https://doi.org/10.1242/jcs.01130>.
- Misgeld, T., Kerschensteiner, M., Bayre, F.M., Burgess, R.W., Lichtman, J.W., 2007. Imaging axonal transport of mitochondria in vivo. *Nat. Methods* 4, 559–561. <https://doi.org/10.1038/nmeth1055>.
- Misko, A., Jiang, S., Wegorzewska, I., Milbrandt, J., Baloh, R.H., 2010. Mitofusins 2 is necessary for transport of axonal mitochondria and interacts with the Miro/Milton complex. *J. Neurosci.* 30, 4232–4240. <https://doi.org/10.1523/JNEUROSCI.6248-09.2010>.
- Muller, F.L., Song, W., Jang, Y.C., Liu, Y., Sabia, M., Richardson, A., Van Remmen, H., 2007. Denervation-induced skeletal muscle atrophy is associated with increased mitochondrial ROS production. *AJP: Regul. Integr. Comp. Physiol.* 293, R1159–R1168. <https://doi.org/10.1152/ajpregu.00767.2006>.
- Nguyen, T.T., Oh, S.S., Weaver, D., Lewandowska, A., Maxfield, D., Schuler, M.-H., Smith, N.K., Macfarlane, J., Saunders, G., Palmer, C.A., Debattisti, V., Koshiba, T., Pulst, S., Feldman, E.L., Hajnóczky, G., Shaw, J.M., 2014. Loss of Miro1-directed mitochondrial movement results in a novel murine model for neuron disease. *Proc. Natl. Acad. Sci.* 111, E3631–E3640. <https://doi.org/10.1073/pnas.1402449111>.
- Palomo, G.M., Granatiero, V., Kawamata, H., Konrad, C., Kim, M., Arreguin, A.J., Zhao, D., Milner, T.A., Manfredi, G., 2018. Parkin is a disease modifier in the mutant SOD1 mouse model of ALS. *EMBO Mol. Med.* 10, e8888. <https://doi.org/10.15252/emmm.201808888>.
- Stowers, R.S., Megeath, L.J., Górski-Andrzejak, J., Meinertzhagen, I.A., Schwarz, T.L., 2002. Axonal transport of mitochondria to synapses depends on Milton, a novel Drosophila protein. *Neuron* 36, 1063–1077.
- Sturtz, L.A., Diekert, K., Jensen, L.T., Lill, R., Culotta, V.C., 2001. A fraction of yeast Cu, Zn-superoxide dismutase and its metallochaperone, CCS, localize to the intermembrane space of mitochondria. A physiological role for SOD1 in guarding against

- mitochondrial oxidative damage. *J. Biol. Chem.* 276, 38084–38089. <https://doi.org/10.1074/jbc.M105296200>.
- Wang, Y., Nartiss, Y., Steipe, B., McQuibban, G.A., Kim, P.K., 2014. ROS-induced mitochondrial depolarization initiates PARK2/PARKIN-dependent mitochondrial degradation by autophagy. *Autophagy* 8, 1462–1476. <https://doi.org/10.4161/autophagy.21211>.
- Yanase, S., Onodera, A., Tedesco, P., Johnson, T.E., Ishii, N., 2009. SOD-1 deletions in *Caenorhabditis elegans* alter the localization of intracellular reactive oxygen species and show molecular compensation. *J. Gerontol. Ser. A Biol. Med. Sci.* 64A, 530–539. <https://doi.org/10.1093/gerona/glp020>.
- Zhang, F., Wang, W., Siedlak, S.L., Liu, Y., Liu, J., Jiang, K., Perry, G., Zhu, X., Wang, X., 2015. Miro1 deficiency in amyotrophic lateral sclerosis. *Front. Aging Neurosci.* 7, 165. <https://doi.org/10.3389/fnagi.2015.00100>.
- Zhu, Y.-B., Sheng, Z.-H., 2011. Increased axonal mitochondrial mobility does not slow amyotrophic lateral sclerosis (ALS)-like disease in mutant SOD1 mice. *J. Biol. Chem.* 286, 23432–23440. <https://doi.org/10.1074/jbc.M111.237818>.